



A method based on neural networks for generating solar radiation map

Z. Ramedani, M. Omid, A. Keyhani

Department of Agricultural Machinery Engineering, Faculty of Agricultural Engineering and Technology, University of Tehran, Karaj, Iran.

Abstract

Estimation of global solar radiation (GSR) is important in most solar energy applications, particularly in design methods, in system characterization and in decision making for energy management. In this paper, a new methodology based on artificial neural networks (ANN) for generating daily GSR data is presented. By modeling GSR in regions where historical records are available, solar potential map for other sites that GSR have not been recorded was generated. In order to examine the ANN models, meteorological data throughout the year 2008 belonging to Karaj city in Alborz province of Iran were used to develop GSR predictors. Input parameters were maximum temperature, relative sunshine duration and extraterrestrial solar radiation while the output parameter was the solar radiation. Various networks were designed and tested and the most accurate model was selected. The best network was found as one hidden layer network with 3-4-1 topology, i.e., a network having four neurons in its hidden layer. To estimate the differences between the measured and predicted values, root mean square error (RMSE), mean absolute error (MAE), mean absolute percentage error (MAPE) and coefficient of determination (R^2) were computed as 0.66, 0.52, 4.46% and 0.978, respectively. The optimum ANN model was then used to predict GSR in other cities in the province. Data from three stations located in Hashtgerd, Taleghan and Chitgar cities were used as production set. The GSR values for production sites of Hashtgerd, Taleghan and Chitgar were calculated as 4.93, 4.35 and 5.08 kWh m⁻² day⁻¹, respectively. Finally, the predicted solar potential values in all stations were integrated and represented in the form of a map. While results are site-specific, the methodology introduced here is general and provides an inexpensive means for GSR prediction based on readily available data.

Copyright © 2012 International Energy and Environment Foundation - All rights reserved.

Keywords: Alborz; Solar radiation; Prediction; Map; Artificial neural networks.

1. Introduction

Iran is located in a sunny belt between 25° and 40° N latitudes, and hence, most of the locations in Iran receive abundant solar energy. Alborz province in north central of Iran has the ability for using this potential. Accurate forecasting of meteorological behaviors mainly solar radiation is required in most solar energy applications, particularly in design methods, in system characterization and in decision making for energy management. Industrial grade devices for measuring solar radiation such as a "pyranometer" are delicate and expensive. This instrument with its extremely absorptive surface senses solar temperature and gives an output voltage related to the amount of solar radiation striking the surface.

It is not feasible to measure the solar resource for all these potential uses; rather, one must use models to calculate the local incident solar radiation.

Over the past decades, several researchers have developed many empirical and physical radiation models for predicting the solar energy potential. Sabbagh [1], Paltridge [2], Daneshyar [3], Hargreaves and Samani [4] and Angstrom [5] are some linear models for this purpose. On the other hand, soft computing techniques are known for their efficiency in dealing with complicated problems when conventional or analytical methods are infeasible or too expensive, with only limited sets of operational data available. These techniques are based on artificial neural networks (ANNs), adaptive neuro-fuzzy inference system (ANFIS) and their developments. There have been a number of studies that have used ANNs to solve problems in meteorology. For example, Luk et al. [6] used three alternative types of ANNs, namely multilayer feed forward neural networks (MLFN), partial recurrent neural networks (PRNN), and time delay neural networks (TDNN) to provide reasonable predictions of the rainfall depth one time-step in advance. Moghaddamnia et al. [7] in a comparative study assessed performance of nonlinear techniques like local linear regression (LLR) multilayer perceptron (MLP), Elman neural network, neural network auto-regressive models with exogenous inputs (NNARX) and ANFIS models to estimate daily (global) irradiation values with the Gamma test.

All of the recent researches about application of ANN in prediction of GSR are focused to determine the best structure [8-10]. Also, some researchers have presented a solar map in their studied region or country [11-13]. In this research, we want to proceed one step forward to that of previous studies. Thus the aims of this study are (1) estimation of solar energy potential in Karaj station using ANNs, and (2) using the best structure of ANN for predicting GSR in other stations of Alborz province. The predicted solar potential values from the ANN in all stations are then given in the form of a map. In other words, this study shows the general perspective of the solar resource in Alborz province and is the first on solar resource prediction in the region (or any region with similar conditions) by using ANN.

2. Artificial neural networks

Artificial neural networks are mathematical models inspired by the organization and functioning of biological neurons. It can be characterized as massively parallel interconnections of simple neurons that function as a collective system. The prediction by a well-trained ANN is normally much faster than the conventional simulation programs or mathematical models as no lengthy iterative calculations are needed to solve differential equations using numerical methods, but the selection of an appropriate neural network topology is important in terms of model accuracy and model simplicity [14]. In structure of ANNs there are three groups of neurons; input, hidden, and output that are placed in input, hidden, and output layers. The layers are connected with a transfer function. Figure 1 is a general architecture of a Feed Forward ANN, with one hidden layer. In back propagation neural networks model during training, inputs and outputs are related by adjusting weights and prediction error is minimized. Most ANNs have three layers or more: an input layer, which is used to present data to the network; an output layer, which is used to produce an appropriate response(s) to the given input, and one or more intermediate layers, which are used to act as a collection of feature detectors [15].

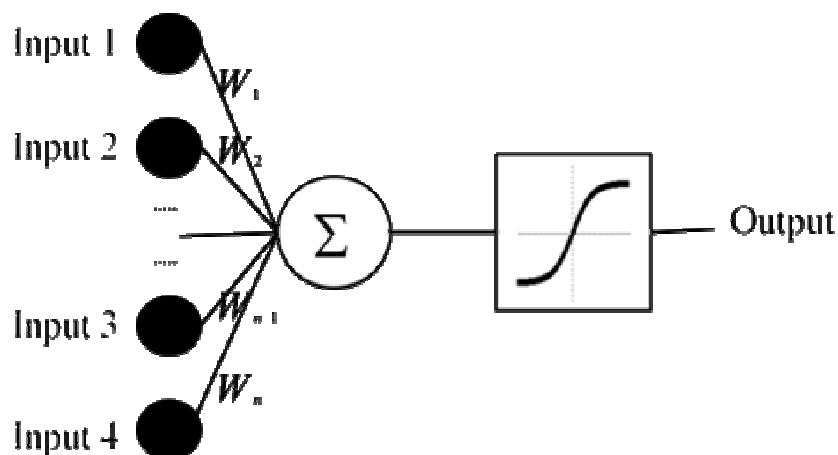


Figure 1. Schematic representation of a simple artificial network model

Building a neural network forecaster for a particular forecasting problem is a nontrivial task that is conducted based on trial and error. Modeling issues that affect the performance of an ANN must be considered carefully. One critical decision is to determine the appropriate architecture, that is, the number of layers, the number of nodes in each layer, and the number of arcs which interconnect with the nodes. Other network design decisions include the selection of transfer functions of the hidden and output nodes, the training algorithm, data transformation or normalization methods, training and test sets, and performance measures [16].

The transfer function determines the relationship between inputs and outputs of a neuron and its network. The logistic sigmoid [Eq (1)], tangent sigmoid [Eq (2)] and purelin transfer functions are used in the neurons of hidden and output layers [17].

$$f(\text{net}_j) = o_j = \frac{1}{1 + \exp(-\text{net}_j)} \quad (1)$$

$$f(\text{net}_j) = o_j = \frac{2}{1 + \exp(-2\text{net}_j)} - 1 \quad (2)$$

where o_j is the output of the j th neuron and net_j is the weighted sum of the inputs. Net is obtained by:

$$\text{net}_j = \sum_{i=1}^v w_{ij} o_i \quad (3)$$

for which net_j is the number of input connections, w_{ij} is a component of the weight vector, and o_i is the input activation of the i th neuron in the preceding layer.

In the feed-forward networks, error minimization can be obtained by a number of procedures including Gradient Descent (GD), with momentum (GDM), Scaled Conjugate Gradient (SCG) and Bayesian Regulation (BR) algorithms. MLPs are normally trained with error back propagation (BP) algorithm. BP uses GD technique which is very stable when a small learning rate is used, but has slow convergence properties [18]. Several methods for speeding up BP algorithm have been developed including adding a momentum term or using a variable learning rate.

In this paper, BP learning algorithm has been used in feed forward with one and two hidden layers. Specifically, three different ANN models using LM, SCG and BR algorithms were developed to predict GSR. In the following we shall refer to these networks as SCG-NN, BR-NN and LM-NN, respectively. Both logistic sigmoid (logsig) as in Eq (1) and tangent sigmoid (tansig) as in Eq (2) transfer functions have been used in hidden layer (s) for each of these training algorithms. A linear transfer function (purelin) transfer function has been used in output layer in all cases. Since the documentation on these algorithms are readily available, only LM algorithm is discussed here.

2.1 Levenberg–Marquardt algorithm

Among variety of training algorithms such as GD, GDM, SCG, LM, and BR algorithms, LM training (trainlm) is more used between researches. It is faster and more accurate than the standard BB algorithm for training. It can converge from ten to one hundred times faster than the standard algorithm using delta rules. This algorithm operates in the batch mode only and is invoked using trainlm function in Matlab. Like the quasi-Newton methods, the LM algorithm was designed to approach a second order training speed without having to compute the Hessian matrix. When the performance function has the form of a sum of squares (as in training feed forward networks), then the Hessian matrix can be approximated as [19]:

$$H = J^T J \quad (4)$$

and the gradient can be computed as [19]:

$$G = J^T e \quad (5)$$

where J is the Jacobian matrix that contains first derivatives of the network errors with respect to the weights and biases and e is a vector of network errors. The Jacobian matrix can be computed through a standard BP technique that is much less complex than computing the Hessian matrix. Accordingly, the LM algorithm uses this approximation to the Hessian matrix in the following Newton-like update [19]:

$$w_{k+1} = w_k - [J^T J + \mu I]^{-1} J^T e \quad (6)$$

where w indicate the weights of neural network, and μ a scalar that controls the learning process. Note that when the parameter μ is large, the above expression approximates GD with a small step size while for a small μ the algorithm approximates the Newton's method. By adaptively adjusting μ , the LM can maneuver between its two extremes: the GD and the Newton's algorithm.

Three different program codes were written in MATLAB language [17] for the BR, LM and SCG-NN simulations. Different ANN architectures were tried using these codes and the appropriate model structures were determined. In the training stage, we used an increased number of neurons (4, 6 and 8) in the single hidden layer case and different numbers of neurons in the two hidden layers (3-2 and 5-3) case to define the output accurately with minimum error. Inputs and outputs are randomized in training and testing periods. There are no acceptable rules to determine the optimum size of the training data set. Here, the dataset was split into the training (76% of the total data – 54 data) and testing (24% – 17 data).

2.2 Statistical analysis

An accuracy measure is often defined in terms of the forecasting error which is the difference between the actual (desired) and the predicted values. There are a number of measures of accuracy in the related literature and the most frequently used are:

$$RMSE = \sqrt{\frac{\sum (e_t)^2}{N}} \quad (7)$$

$$MAE = \frac{\sum |e_t|}{N} \quad (8)$$

$$MAPE = \frac{1}{N} \sum \left| \frac{e_t}{y_t} \right| \times 100 \quad (9)$$

$$R^2 = 1 - \frac{\sum e_t^2}{\sum y_t^2} \quad (10)$$

where e_t is the individual forecast error; y_t is the actual value; and N is the number of error terms.

A model is often selected from a wide class of models by optimizing a statistical indicator such as coefficient of determination (R^2) in Eq (10). The decision about the quality of each approach (algorithm, number of hidden layers and neurons) is made using some error criteria, which are given in Eqs (7)-(9). R^2 approaching 1 and RMSE, MAE and MAPE approaching zero indicate that the solution of the problem gives the most accurate answers. Inputs and outputs are randomized in training and testing periods. Among the studied algorithms, BR-NN using tansig activation function performed slightly superior than LM and SCG algorithms. The best BR-NN results were obtained for 4 neurons in the hidden layer. Therefore, the 3-4-1 topology was selected as optimum model for predicting GSR.

3. Study area and data set

Despite of the large spectrum of applications demanding solar radiation data, such direct measurements of solar energy are not widely available, rendering the use of numerical techniques essential alternatives. With such indirect techniques, other observed meteorological data are mathematically exploited in order to estimate the amounts of GSR reaching the earth. Except GSR, other meteorological data are parameters that are routinely recorded at a large number of climatological stations (manned and automatic), due to the low cost of the respective recording instrumentation and the easiness of data acquisition.

The Alborz province with an area of 5833 square km was selected as the study area located between 25 and 40° N latitudes and 52° West longitude, in the north central of Iran. Measured daily data for the full year of 2008 were collected from the Islamic Republic of Iran Meteorological Office data center in Karaj, Hashtgerd, Taleghan and Chitgar stations [20]. Chitgar is a city in the west of Tehran province and the climatological characteristics of this region are similar to other cities in Alborz province. Therefore, we have included the data in this region in the simulation. Some of geographical parameters in these stations are shown in Table 1. Also, in this table the cities used for training, testing and production data are indicated separately. The cities selected can give a general idea about solar radiation values of Alborz province. Due to lack of measuring devices, GSR is measured only in Karaj station of Alborz province. In this study, estimation of GSR in other regions is based on meteorological and geographical data and carried out by assistance of best structure of ANN.

The yearly average solar radiation in the Karaj region that is the only solar radiation measurement station in Alborz province is 4.84 kWh m⁻² day⁻¹ [21]. The monthly mean daily temperature ranged from a minimum of 2.2 °C in January and a maximum of 28.4 °C in July [20]. The area gets sufficient bright sunshine hours throughout the year. The average bright sunshine hours are about 8–9 h per day. In Figure 2 mean sunshine durations for these locations are presented. The data sets contain daily information of temperatures (°C), sunshine duration (h) and solar radiation (MJ m⁻² day⁻¹). In this study, the following input parameters have been considered into the model: horizontal extraterrestrial radiation (R_a) [22], maximum air temperature, sunshine duration and daylight hours. The training and validation data sets were selected by the randomization of the input data.

Table 1. Site geographic coordinates and data information

Site	Latitude	Longitude	Elevation (m)	Clear-sky (R_{so})	Record period	Data type
Karaj	35° 55'	50° 54'	1312.5	0.776	2008	Train & Testing
Hashtgerd	36° 0'	50° 45'	1100	0.772	2008	Production
Taleghan	36° 10'	50° 46'	1857	0.787	2008	Production
Chitgar	35° 44'	51° 10'	1305.2	0.776	2008	Production

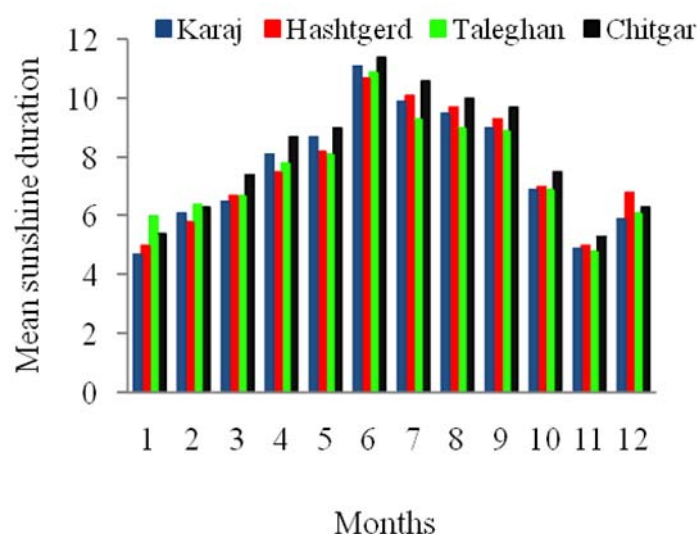


Figure 2. Mean sunshine duration for selected stations

Daylight hours (h), extraterrestrial radiation ($\text{MJ m}^{-2} \text{ day}^{-1}$) are two daily parameters that affect the solar radiation. The extraterrestrial solar radiation that is the solar radiation received at the top of the earth's atmosphere on a horizontal surface, for each day of the year and for different latitudes can be estimated by [22]:

$$R_a = \frac{24 \times 60}{\pi} [\omega_s \sin(\varphi) \sin(\delta) + \cos(\varphi) \cos(\delta) \sin(\omega_s)] G_{sc} d_r \quad (11)$$

where R_a is the extraterrestrial radiation ($\text{MJ m}^{-2} \text{ day}^{-1}$), G_{sc} is solar constant that is equal to $0.0820 \text{ MJ m}^{-2} \text{ min}^{-1}$, d_r is the inverse relative distance of earth-sun (dimensionless), ω_s is the sunset hour angle (rad), φ latitude (rad) that is positive for the northern hemisphere and negative for the southern hemisphere, and δ is the solar declination angle (rad). The expressions for d_r , δ , ω_s and N (daylight hours) are given by Eqs. (A-1) to (A-4) in Appendix A, respectively.

In this study, by using three indicators namely R_a , clear-sky (R_{so}) and relative sunshine duration, quality control of data was carried out. The expression for R_{so} is given as [22]:

$$R_{so} = (0.75 + 2 \times 10^{-5} z) R_a \quad (12)$$

where z is the site altitude. In Karaj city for $z=1312.5 \text{ m}$, $R_{so} = 0.776 R_a$. The values of R_{so} for other cities (Hashtgerd, Taleghan and Chitgar) are given in Table 1.

The relative sunshine duration is a ratio that expresses the cloudiness of the atmosphere. It is the ratio of actual sunshine duration (n) to the daylight hours or maximum sunshine duration (N). Relative sunshine duration is in the range of 0-1. This ratio is equal to one when the whole sky is sunny, e.g. $n=N$. The data for the day for which any of the following occurs, were excluded from the training and cross validation and testing data sets whenever:

- (I) there was missing data;
- (II) solar radiation was greater than R_a ;
- (III) solar radiation was greater than R_{so} ;
- (IV) sunshine duration was higher than daylight hours;
- (V) sunshine duration to daylight hours ratio was lower than 0.3^8 ;

Therefore, only correctly measured data were used in the model.

4. Results and discussion

For building different ANNs the input nodes were maximum temperature, relative sunshine duration and extraterrestrial solar radiation, while the output was GSR. Hidden nodes with appropriate nonlinear transfer functions were used to process the information received by the input nodes. This network can be written mathematically as:

$$GSR = b_0 + \sum_{j=1}^n v_j f \left(\sum_{i=1}^m w_{ij} O_i + b_{0j} \right) \quad (13)$$

where GSR is the estimated value of the daily GSR, m is the number of input nodes, n is the number of hidden nodes, $f(\cdot)$ is a sigmoid transfer function, w_{ij} ($i = 1, 2, \dots, m; j = 0, 1, \dots, n$) are weights from the input to hidden nodes ($i \rightarrow j$), and v_j is a vector of weights from the hidden to output nodes. b_{0j} and b_0 are bias terms in the hidden and output nodes, respectively.

The performance of the various neural networks for modeling solar radiation in Alborz province was examined. Karaj is the only meteorological station in this province that has GSR measured instruments. For this purpose different ANNs with variant of training algorithms (LM, BR and SCG), transfer functions (logsig and tansig), and hidden layers and nodes were constructed using Karaj meteorological data. The statistical error values such as the RMSE, MAE, MAPE and R^2 were used to select the best

model. The results are given in Table 2. This station is used both for training and testing ANN models. For training phase, the BR-NN with 3-4-1 topology (bolded in Table 2) seems to perform slightly better than the LM-NN and SCG-NN. From this table it is indicated that the best structure of ANN model uses BR training algorithm (BR-NN), tangent sigmoid transfer function in input layer and 4 neurons in its hidden layer. For the optimal network (3-4-1 topology) Eq (12) can be written more precisely. For this network, $m=3$ and $n=4$. We have tangent sigmoid transfer function (tansig), $f(x) = \tanh(x)$ (as given by Eq (2)) for the hidden layer neurons. In the output layer, the outputs of the hidden layer are summed linearly using purelin ($f(x) = x$) to produce GSR as it is desired for forecasting problems. The weights and biases for this model are given below:

$$W_{ij} = \begin{bmatrix} 0.0413 & -3.1986 & -0.2400 \\ -0.0416 & 0.0244 & 0.2224 \\ -0.3225 & -0.0156 & -0.0573 \\ -0.0497 & -0.4430 & -0.0396 \end{bmatrix}$$

$$V_j = [-4.6907 \quad 4.6335 \quad -4.0940 \quad -4.1585]$$

$$b_{0j} = [7.6116 \quad -2.3666 \quad -0.0043 \quad 0.8656]^T$$

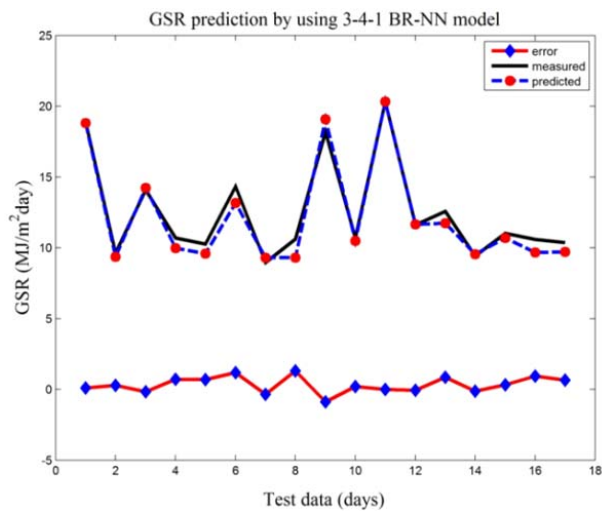
and $b_0 = 4.0945$. Similar expressions, as in Eq (12), can be given for other ANNs.

Performance of optimum BR-NN model analyzed herein was also shown in Figure 3(a). For the testing phase, it can be seen from this figure, the BR-NN performance was quite satisfactory in prediction of GSR values in Karaj station as it is close to the exact fit line (with $R^2=0.978$). Figures. 3(b) and 3(c) show performance of best structure of each LM (with $R^2=0.973$) and SCG (with $R^2=0.97$) algorithms, respectively. It can be seen from these figures that they are all similar in trend and their obtained statistical indicators verify this point. As shown in Table 2, the RMSE, MAE and MAPE for these models range from 0.6 to 2.11, from 0.52 to 1.53 and from 4.39% to 11.45%, respectively. The performance measures for the best model (3-4-1 topology) for MSE, MAE and MAPE are 0.66, 0.52 and 4.46%, respectively. Figure 4 shows structure of this topology. Comparison between this study and other published literature on similar research which used ANN for predicting GSR reveals that this model in statistical indicators is more successful. For example, the MAPE values in this study are better than those of Behrang et al. [9] and Azadeh et al. [23]. Also the RMSE values are better than those of Tymvios et al. [8], Azadeh et al. [23], Bocco et al. [24] and Rahimikhoob [25].

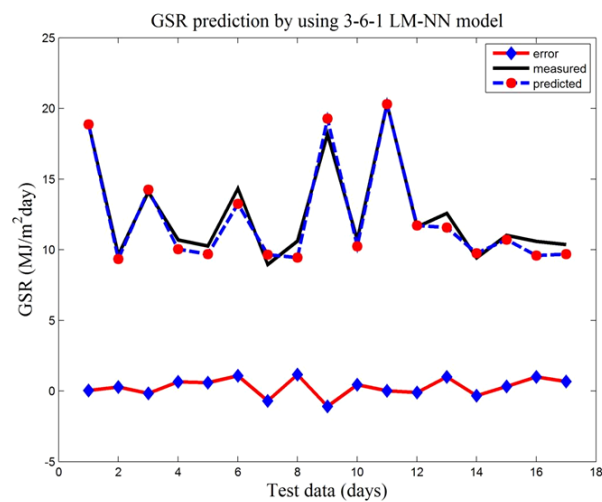
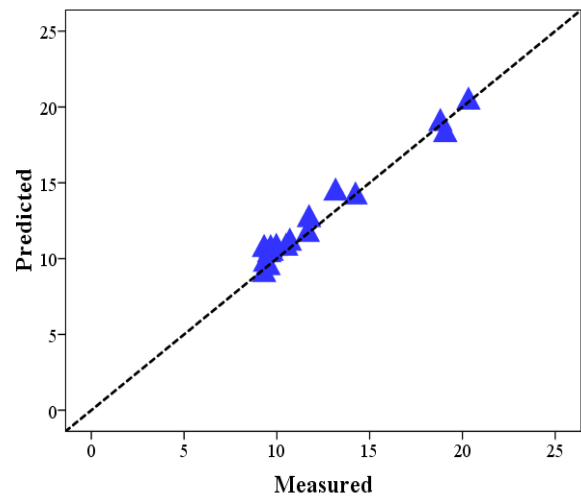
In the present research we will go one step further to predict the solar radiation data for places that GSR data are not available. Having selected the best ANN model for this site, data from other stations were then used as production sets for predicting GSR and generating a map. These sites are located in Hashtgerd, Taleghan and Chitgar cities. The predicted solar energy potential of Alborz using the ANN model is given in Figure 5 as yearly maps, i.e., in a form suitable for scientists investigating the solar energy potential. For generating this map, inputs (maximum temperature, relative sunshine duration and extraterrestrial solar radiation) from these sites as production set, as well as weights and biases matrices were used inside Eq (12) to find the corresponding GSRs of the remaining three sites. The yearly average GSR values for production sites of Hashtgerd, Taleghan and Chitgar were estimated as 4.93, 4.35 and 5.08 kWh m⁻² day⁻¹, respectively.

Table 2. Performace of various ANN topologies for estimating GSR in Karaj

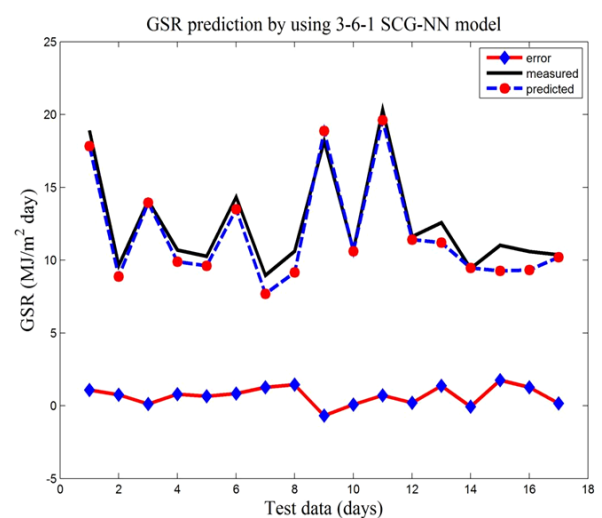
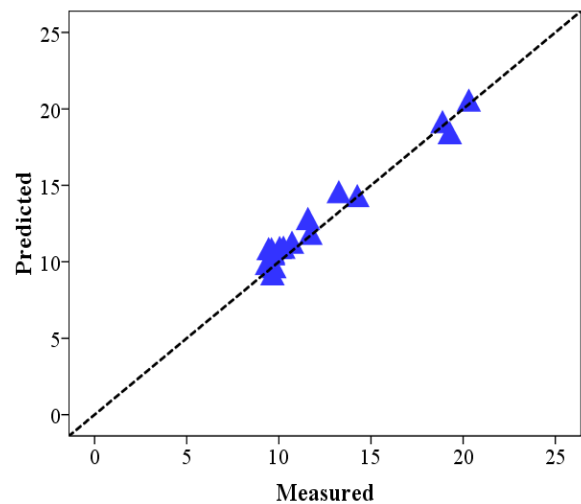
Algorithm	Transfer Function	Neurons ($N_{h1} + N_{h2}$)	RMSE	MAE	MAPE (%)	R^2
LM	logsig	4	0.73	0.64	5.61	0.966
LM	logsig	6	0.74	0.69	6.12	0.965
LM	logsig	8	0.73	0.57	4.9	0.967
LM	logsig	3+2	2.11	1.53	11.45	0.623
LM	logsig	5+3	0.83	0.70	6.22	0.966
LM	tansig	4	0.73	0.63	5.51	0.966
LM	tansig	6	0.68	0.57	4.94	0.973
LM	tansig	8	0.77	0.65	5.61	0.956
LM	tansig	3+2	1.32	1.1	9.26	0.855
LM	tansig	5+3	0.73	0.62	5.54	0.967
BR	logsig	4	0.67	0.53	4.57	0.977
BR	logsig	6	1.68	1.26	9.1	0.779
BR	logsig	8	1.68	1.29	9.48	0.777
BR	logsig	3+2	0.67	0.54	4.66	0.972
BR	logsig	5+3	0.71	0.65	5.75	0.967
BR	tansig	4	0.66	0.52	4.46	0.978
BR	tansig	6	1.66	1.22	8.7	0.798
BR	tansig	8	1.16	0.89	6.46	0.903
BR	tansig	3+2	0.60	0.52	4.47	0.974
BR	tansig	5+3	0.68	0.55	4.63	0.969
scg	logsig	4	1.22	1.00	8.29	0.910
scg	logsig	6	0.73	0.59	4.85	0.967
scg	logsig	8	1	0.86	7.39	0.940
scg	logsig	3+2	1.72	0.95	7.53	0.883
scg	logsig	5+3	1.12	0.90	8.08	0.909
scg	tansig	4	0.69	0.53	4.39	0.962
scg	tansig	6	0.79	0.66	5.59	0.970
scg	tansig	8	0.64	0.53	4.69	0.968
scg	tansig	3+2	1.15	0.96	7.89	0.935
scg	tansig	5+3	1.07	0.89	7.17	0.935



(a)



(b)



(c)

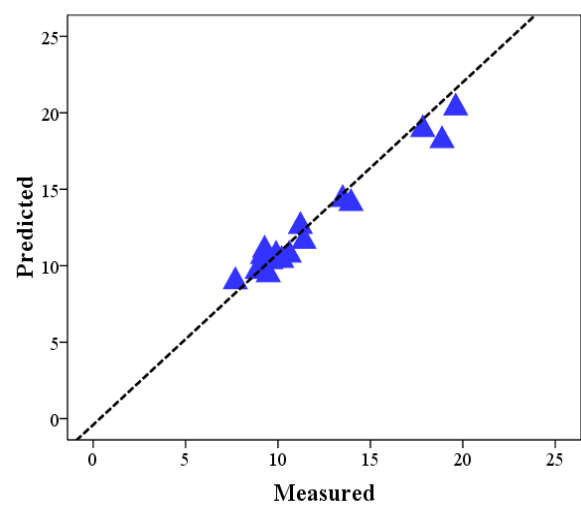


Figure 3. The results of comparison between measured and predicted GSR by using (a) 3-4-1 BR-ANN model (b); 3-6-1 LM-NN model and (c) 3-6-1SCG-NN model for testing data set in Karaj station

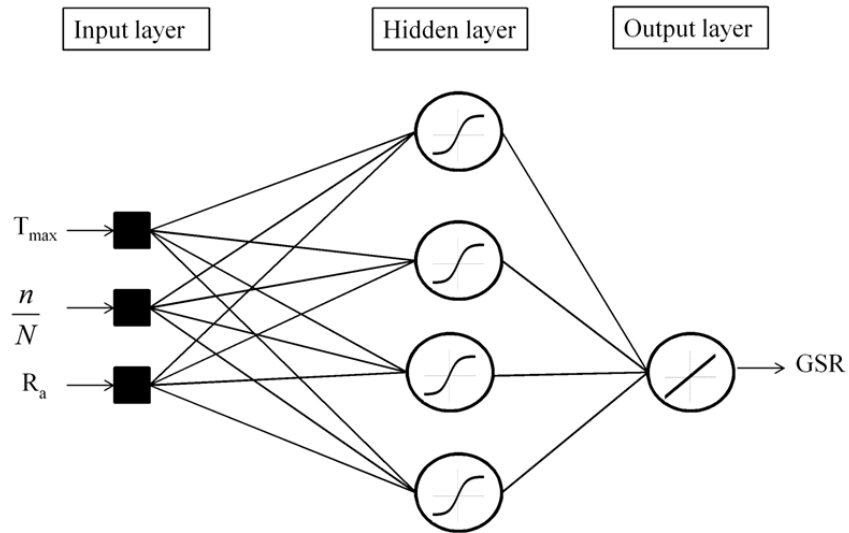


Figure 4. Best ANN topology for prediction GSR map in Alborz province

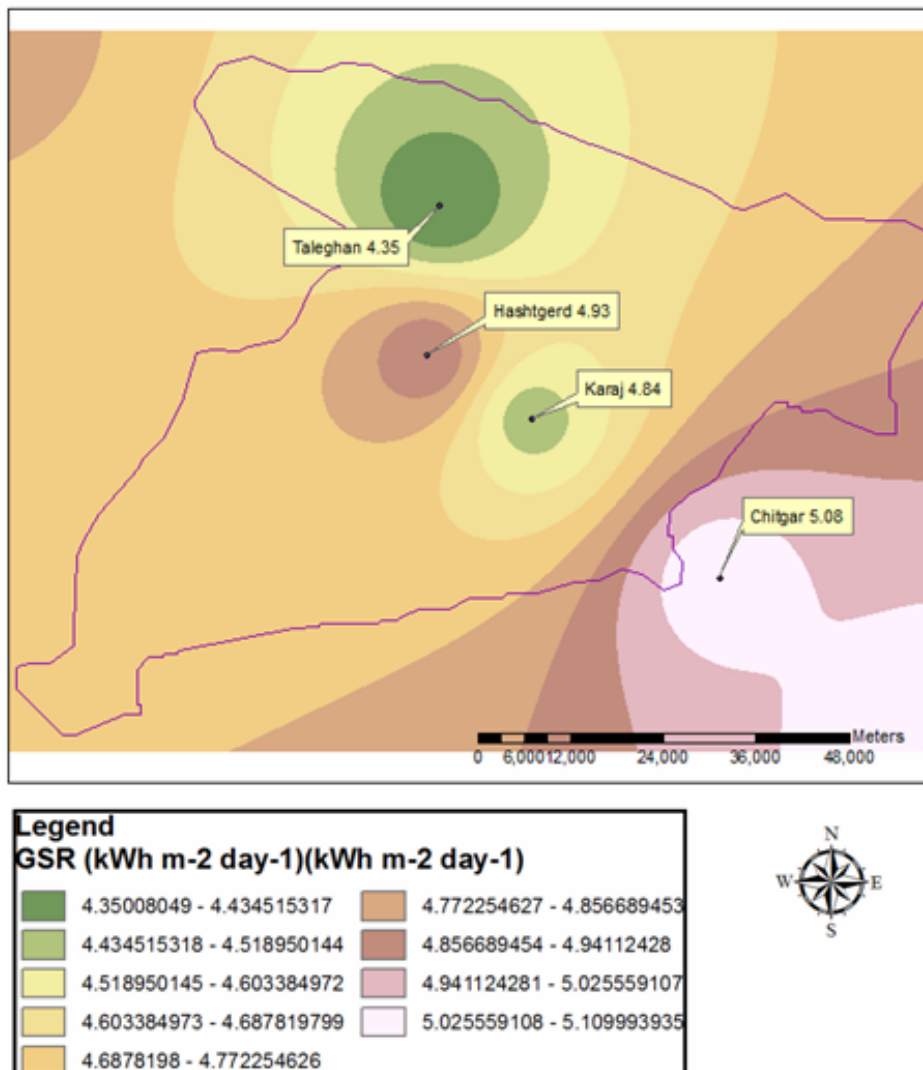


Figure 5. Predicted solar potential (kWh m⁻² day⁻¹) in Alborz province for year 2008

5. Conclusion

An artificial neural network model was developed that could be used to estimate solar radiation on a horizontal surface for locations in Karaj and other cities with similar climate and terrain. The ANN architecture designed is a feed forward back-propagation with one-hidden layer containing four neurons with tangent sigmoid as the transfer function. The output layer utilized a linear transfer function. The training algorithm used was the Bayesian Regulation algorithm and the input variables to the ANN model were relative sunshine duration, extraterrestrial solar radiation and maximum temperature. The proposed ANN model was then used for predicting daily global solar radiation in other regions with similar climate and terrain as in Karaj station. Finally, the solar map for the studied area was produced. Although the results presented here are site-specific, the adopted methodology is rather general and provides an inexpensive and simple means for predicting GSR based on readily available data.

Appendix

The inverse relative distance of earth-sun, d_r , and solar declination, δ , are given by Eq. (A1) and Eq. (A2), respectively²²:

$$d_r = 1 + 0.033 \cos\left(\frac{2\pi}{365} J\right) \quad (\text{A1})$$

$$\delta = 0.409 \sin\left(\frac{2\pi}{365} J - 1.39\right) \quad (\text{A2})$$

where J is the number of the day in the year between 1 (January 1st) and 365 or 366 (December 31st). Also, the sunset hour angle, ω_s , and daylight hours, N , are given by Eq. (A3) and Eq. (A4), respectively [22]:

$$\omega_s = \arccos(-\tan \varphi \tan \delta) \quad (\text{A3})$$

$$N = \frac{24}{\pi} \omega_s \quad (\text{A4})$$

Acknowledgements

The financial support provided by the Research Department of University of Tehran, Iran, is duly highly acknowledged.

References

- [1] Sabbagh J., Sayigh A.A.M., Al-Salam E.M.A. Estimation of the total solar radiation from meteorological data: Solar Energy. 1977; 19, 307–318.
- [2] Paltridge G.W., Proctor D. Monthly mean solar radiation statistics for Australia: Solar Energy. 1976, 18, 235–243.
- [3] Daneshyar M. Solar radiation statistics for Iran: Solar Energy. 1978, 21, 345–349.
- [4] Hargreaves G.H., Samani Z.A. Estimating potential evapotranspiration: Journal of Irrigation and Drainage Engineering, ASCE. 1982, 108(IR3), 223–53.
- [5] Angstrom A. Solar and terrestrial radiation: Quarterly Journal of the Royal Meteorological Society. 1924, 50, 121–125.
- [6] Luk K.C., Ball J.E., Sharma A. An application of artificial neural networks for rainfall forecasting: Mathematical and Computer Modeling. 2011, 33, 683–693.
- [7] Moghaddamia A., Remesan R., Hassanpour Kashani M., Mohammadi M., Han D., Piri J. Comparison of LLR, MLP, Elman, NNARX and ANFIS Models-with a case study in solar radiation estimation. Journal of Atmospheric and Solar-Terrestrial Physics. 2009, 71, 975.
- [8] Tymvios F.S., Jacovides C.P., Michaelides S.C., Scouteli C. Comparative study of Angstrom's and artificial neural networks methodologies in estimating global solar radiation: Solar Energy. 2005, 78, 752–762.

- [9] Behrang M.A., Assareh E., Ghanbarzadeh A., Noghrehabadi A.R. The potential of different artificial neural network (ANN) techniques in daily global solar radiation modeling based on meteorological data: *Solar Energy*. 2010, 84, 1468–1480.
- [10] Ramedani Z., Omid M., Keyhani A. Modeling solar energy potential in Tehran province using artificial neural networks: *Green Energy*. 2012, Accepted paper.
- [11] A. Sozen, E. Arcaklioglu and M. Ozalp. Estimation of solar potential in Turkey by artificial neural networks using meteorological and geographical data: *Energy Conversation and Managment*. 2004, 45, 3033–3052.
- [12] Hontoria L., Aguilera J., Zufira P. An application of the multilayer perceptron: Solar radiation maps in Spain. *Solar Energy*. 2005, 79, 523–530.
- [13] Senkal O. Modeling of solar radiation using remote sensing and artificial neural network in Turkey: *Solar Energy*. 2007, 81, 692–95.
- [14] Barma S.D., Das B., Giri A., Majumder S., Bose P.K. Back propagation artificial neural network (BPANN) based performance analysis of diesel engine using biodiesel: *Journal of Renewable and Sustainable Energy*. 2011, 3, 013101.
- [15] Sudheer K.P., Gosain A.K., Rangan D.M. Saheb S.M. Modelling evaporation using an artificial neural network algorithm. *Hydrol Process*. 2002, 16, 3189–3202.
- [16] Zhang G., Patuwo B.E., Hu M.Y. Forecasting with artificial neural networks: the state of art: *international journal of forecasting*. 1998, 14, 35–62.
- [17] MATLAB 7.8.0, R2009 Service Pack, Mathworks, Inc., 2009.
- [18] Omid M., Mahmoudi A., Omid M.H. An intelligent system for sorting pistachio nut varieties. *Expert Systems with Applications* 2009. *Expert System with Application*. 2009, 36, 11528–11535.
- [19] Omid M., Mahmoudi A., Omid M.H. Development of pistachio sorting system using principal component analysis (PCA) assisted artificial neural network (ANN) of impact acoustics: *Expert System with Application*. 2010, 37, 7205–7212.
- [20] Islamic Republic of Iran Meteorological Office (IRIMO). Data Center, Tehran, Iran, 2008.
- [21] Surface meteorology and solar energy (SSE). NASA renewable energy resource website, <http://eosweb.larc.nasa.gov/sse/RETScreen>, 2011.
- [22] Anonymous, Food and Agricultural Organization (FAO). www.fao.org, 2008.
- [23] Azadeh A., Maghsoudi A., Sohrabkhani S. An integrated artificial neural networks approach for predicting global radiation: *Energy Conversion and Management*. 2009, 50, 1497–1505.
- [24] Bocco M., Willington E., Arias M. Comparison of regression and neural networks models to estimate solar radiation: *Chilean Journal of Agricultural Research*. 2010, 70(3), 428–435.
- [25] Rahimikhoob A. Estimating global solar radiation using artificial neural network and air temperature data in a semi-arid environment: *Renewable Energy*. 2010, 35, 2131–2135.

Z. Ramedani was born in 1986 in Gorgan/Iran, received his B. Sc. degree in Agricultural Mechanization Engineering from the University of Tehran, Iran, in 2009. He is now M.Sc. student in Agricultural Mechanization Engineering in University of Tehran under supervision of Dr. Mahmoud Omid. His main research interests are solar energy and solar thermal systems.
E-mail address: zeynabamedani@ut.ac.ir

M. Omid was born in Yazd/Iran, received his B. Sc degrees in Electronics Engineering from University of Newcastle, Newcastle Upon-Tyne; UK in 1989. Also he received M. Sc. and Ph.D. degree in Telecommunication Engineering from University of Electro-Communications, Tokyo; Japan in 1997. He is currently a Professor in Department of Agricultural Machinery Engineering in University of Tehran. His current research interests are Electronics, Machine Vision, design, management, control and automation of greenhouse, energy modeling and optimization and renewable.
E-mail address: omid@ut.ac.ir

A. Keyhani was born in Yazd/Iran, received his B.Sc. and M.Sc. degrees in Agricultural Machinery Engineering from the University of Tehran, Iran. Also he received Ph.D. degree in Agricultural Engineering from University of Saskatchewan, Canada. He is currently a Professor in Department of Agricultural Machinery Engineering in University of Tehran. His current research interests are Renewable Energies, Agricultural Mechanization, Tillage and Traction.
E-mail address: akeyhani@ut.ac.ir